Enhanced Hydrophobic Double-Layer Nanofibers Membranes for Direct Contact Membrane Distillation

Nawras N. Safi[1*], Basma I. Waisi[1]

[1] Department of Chemical Engineering, College of Engineering, University of Baghdad, Baghdad, Iraq
* Corresponding author's e-mail: nawras.safi1507d@coeng.uobaghdad.edu.iq

ABSTRACT

There are several uses for electrospun nanofiber membranes because of their unique properties. Electrospinning, under suitable conditions, has allowed for the successful fabrication of nanofibrous membranes. This research, a dual-layer membrane was prepared and applied in a direct contact membrane distillation (DCMD) system. Polyacrylonitrile (PAN) based electrospun nanofibers comprised the initial (base) layer. Hydrophobic electrospun nanofibers made from polymethyl methacrylate (PMMA) comprised the second (top) layer. The analysis was carried out using contact angle measurements and scanning electron microscopy (SEM) for the morphology and wetting of a series of two-layer nanofiber membranes that were made with different percentages of PAN: PMMA. The study examined how the permeate flux was affected by changes in feed concentration, feed temperature, and feed flow rate. and optimized within a logical framework. These included feed inlet temperatures between 35 and 55 °C, salt concentrations between 70,000 and 210,000 ppm, and rates of supply flow of 0.2, 0.4, and 0.6 L/min. DCMD findings for the (25 PAN:75PMMA) membrane displayed that the amount of salt it rejected was better than 99.356% with flux 51.872 kg/m²·h and a penetrate through conductivity lower down 334 µs/cm when performed under optimally supplied conditions (i.e., 70 g/L; 0.6 L/min; and 55 °C).

Keywords: desalination, hydrophobic electrospun nonwoven nanofibers, direct contact membrane distillation.

INTRODUCTION

The purity of our drinking water is paramount, and there is widespread concern about its safety in the modern world (Kayvani fard and Manawi 2014). The demand for and the supply of fresh water has increased continuously over the past two decades, making this problem increasingly important in relation to the alarmingly high rate at which the water shortage is predicted to increase by 2025 (Alkhudhiri et al. 2012). The membrane separation technique has shown the most promise and applicability in the desalination field during the past few decades, more renewable and cost-effective processes due to its high performance (Rashad 2022). Membrane processes are easy to scale up because of their compact and modular nature devices with the potential for selective component transfer, low energy consumption, moderate operation temperatures, and simple

product treatment (Hameed 2013). The key benefit of membrane technology over conventional distillation techniques is the membrane's ability to be applied at low input temperatures and lower pressure than membrane processes dependent upon pressure, such as reverse osmosis (Cheng et al. 2016). By using the membrane process, the substances and molecules are effectively excluded by the membrane, resulting in separating the inlet into two solutions: product and concentrate (Al-Alawy and Al-Musawi 2013, Majeed 2016). In many regions in developing countries that experience water scarcity cannot afford the expensive conventional desalination technologies (Khalaf and Hassan 2019). Thus, a need for a low-cost desalination process that still yields potable water has prompted research into membrane distillation (MD). When the aqueous solution is heated to a suitable temperature, the MD process begins as the solution evaporates along on the side of the hot

feed that is near to the membrane. The pressure differential between the membrane's two sides is created by the gradient of temperature across the membrane, which drives a stream of water vapor via the dry pores in the membrane and into liquid form in a chilly region (Eleiwi et al. 2016). Micro-porous membranes were used in MD, and the membrane's pores may be hydrophobic, meaning they reject water. They had be thermally stable, resistant to chemicals, and have a low resistance to mass transfer. Due to its non-wettability by aqueous feeds, the hydrophobic polymer has been a popular choice for use as a membrane material in membrane distillation (Shukla et al. 2015). Although inexpensive, polymer membranes benefit from low surface porosity and permeability due to their asymmetrical construction (Wang et al. 2012).

Recently, electrospun nanofiber polymeric membranes (ENMs) have been widely used in nonwoven electrospun nanofibers form because of their unique advantages, including high permeability and surface area (Sabeeh and Waisi 2022). Electrospinning is an effective approach for producing Using an electrostatic field on nonwoven nanofibers of varied sizes, and it can be used to create nonwoven nanofibers (Waisi 2019, Heikkilä and Harlin 2008). Scientists have already used electrospun nanofibers in several promising fields, including tissue engineering (Francis et al. 2010), indoor air purification (Sheraz et al. 2023), oil/water separation (Li et al. 2022), organic solar cells (Haghighat Bayan et al. 2021), and in wastewater treatment and waste reduction, particularly in uses where the recovered materials are highly valuable, such as recycling coolants and aqueous cleansers used in machining (Cheryan and Rajagopalan 1998).

In addition, ENMs membranes were applied in seawater desalination (Woo et al. 2021). Nanofibrous membranes produced by electrospinning exhibit very porous, with big pores, a very narrow distribution of pore sizes, and a very large surface area. Those qualities are essential if you want your MD process to generate a lot of water vapor. Hybrid composite membranes made of electrospun nanofibers for effective antimicrobial action using polyacrylonitrile (PAN) nanofibers membranes (Shalaby, et al. 2018). Also membrane distillation using electrospun polyvinylidene fluoride (PVDF) fabrics (Hu et al. 2022). For desalination during membrane distillation, electrospun polyamide fiber membranes that have been surface fluorinated employing chemical

vapor deposition of poly(1H,1H,2H,2H-perfluorodecyl acrylate) (PPFDA) (Guo et al. 2015). For the purpose of treating highly salinized wastewater from industries using membrane distillation with omniphobic Hydrothermal fabrication of a nanofibrous membrane from polyvinylidene fluoride-co-hexafluoropropylene (PVDF-HFP) nanofibers (Li et al. 2019), Membrane distillation with electrospun omniphobic membranes containing polydopamine and polyethylenimine (PDA/PEI) for the treatment of hypersaline effluent from the chemical industry (Meng, et al. 2023).

A double-layer PAN: PMMA nonwoven nanofiber membrane was created by electrospinning two layers of nonwoven nanofiber: one made of polymethyl methacrylate (PMMA) on top the other of polyacrylonitrile created to determine the pore size suitability non-wettability for MD application and may be hydrophobic and excellent chemical resistance. To achieve high rejection and low conductivity, the manufactured nanofibers membranes were used in DCMD applications and assessed using the water contact angle (WCA) and scanning electron microscopy (SEM).

MATERIALS AND METHODS

Materials

Membrane production has made use of materials with a molecular weight of 150,000 g/mole of PAN and 350,000 g/mole of PMMA. PMMA and PAN were selected because of their great heat and chemical resistance, abrasion, aging, and better thermal and chemical stability. PMMA and PAN can be dissolved in N, N-dimethylformamide (DMF) (density = 0.948 g/cm³) and for four hours while stirring continuously at 50 °C. NaCl, or sodium chloride, was utilized to make the salt water. The German chemical supplier Sigma-Aldrich was used for all of our purchases.

Membranes fabrication

The electrospinning method yielded a PAN-based nonwoven nanofibers membrane, where polymer droplets are stretched to reduce surface tension in an electric field. The solutions of polymeric were initially made through dissolving a predetermined polymer quantity in DMF that have been mixed repeatedly for five hours in order to prepare at 40 °C. After that, the dope

solution was degassed to get removal of any remaining air bubbles. After that, a plastic syringe was used to transfer the precursor solution, and the syringe pump was turned on. Afterward, a 0.7 mm inner diameter metal needle was connected to the syringe's nozzle. After that, a high voltage was used to force 2 mL/h of polymeric nanofiber through the metal needle and onto the spinning drum (at a speed of 130 rpm).

Nanofiber membranes made from PAN (10 wt%) and PMMA (30 wt%) were the most common. The remaining nanofiber membranes were double-layers of PAN: PMMA (75:25, 50:50, and 25:75) in varying proportions. The first step in making PAN-based nanofiber membranes for nonwoven applications was to spin a specific amount of a PAN/DMF solution 10 wt%. The top layer was made by spinning nonwoven nanofibers a 30 wt% PMMA/DMF precursor solution at 25 kV.

Each membrane was spun with an identical needle-to-collector distance of 15 cm, rate of injection flow of 2 mL/hr, and collector the rate of 130 rpm. All the synthetic fibers were made at room temperature and humidity between 20% and 30%. Each membrane produced had a fiber size between 200 and 1000 nm. The electrospinning method, which involves a high-voltage pulling force acting on polymer droplets 22–25 kV electrostatic field, was ulitized to generate all of the membranes made of nanofibers used here. A metal needle, a syringe filled with typically, an electrospinning system consists of a polymer solution, a voltage power source, and a collector. (Al-Furaiji et al., 2020, Waisi et al., 2019).

Preparation of NaCl solution

To make the brine (feed solution), 70, 140, and 210 grams of Annular (sodium chloride NaCl, M 58.44, Didactic) were measured out using a delicate balance (Kern-PLE 310-3N). One liter of distilled water was used to dissolve the samples, and a magnetic stirrer (MR Hei. Standard) combined the liquids completely. Electric conductivity in distilled water and other solutions can be measured using this meter (Model DDS 307).

Characterizing membranes

In this section, a thorough characterization was carried out using several methods. Before and after chloride alsodium (NaCl) removal, the surface structure and morphologies of pure PAN, pure PMMA, and double-layers of PAN: PMMA nonwoven nanofiber membranes were seen. The membranes' structural morphology is often analyzed using a scanning electron microscope (W. Zhou 2006). SEM pictures of the fibers were used to determine their size distributions and typically their average diameter by taking 20 fiber diameter measurements for each membrane sample.

These measurements were performed with Image J (National Institutes of Health, USA. It is possible to examine the hydrophobicity of the membranes' surfaces by measuring water droplet contact angles as measured by a contact angle analyzer (Theta Lite TL-101).

Experimentation methods (DCMD efficiency)

Figure 1 shows the experimental membrane distillation in direct contact (DCMD) setup. The DCMD carry out study only had around a 5-hour run time. In the DCMD method, the feed hot solution was injected using a peristaltic pump. into the top side of the flat sheet-produced membrane at a flow rate regulated by a control valve and pressure gauge on the right side of the membrane. The cold distillate water and the vapor water circle in the bottom side of the module via a peristaltic pump at a flow rate controlled by a control valve with and pressure gauge on the left side, while the vapor water can pass through the membrane due to the partial pressure driving force at the sides of the membrane. A hand-carried English-made pump, chiller, and bath. The prepared seawater was stored in a 500 mL glass tank and heated in a water bath to various temperatures, from 35 to 65 °C. According to Figure 2, the DCMD Flat sheet membrane module was developed and built in Italy with a size of roughly 6×6 cm^2. The module is constructed from high-heat-resistance silicones impervious to corrosion from the NaCl solution. To give you an idea of scale, each compartment is 4 cm long, 4 cm wide, and 2 mm thick.

Within the direct contact module, the flow pathways were parallel. Figure 1 depicts the results of the heating control system's measurements of the feed streams' inlet and output temperatures. The constant change in the distilled water in the measuring cylinder was monitored to analyze the collected permeate volume throughout the DCMD operation. Distilled water was reused in the feed tank to maintain a steady salinity in the feed solution.
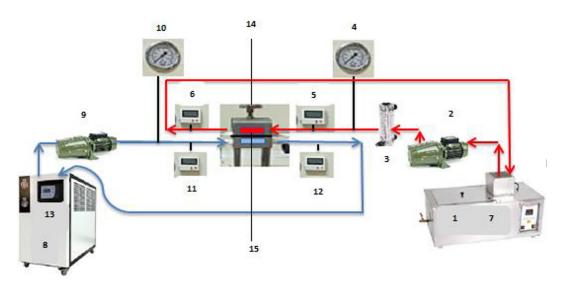
Figure 1. The experimental setup for the DCMD process, 1 – bath for feed, 2 – pump for feed, 3 – rotameter for feed, 4 – inlet pressure gauge for feed, 5 – inlet temperature sensor for feed; 6 – outlet temperature sensor for feed, 7 – tank for feed, 8 – chiller for permeate, 9 – pump for chiller (permeate), 10 – inlet pressure gauge for permeate, 11 – sensor for the inlet temperature for permeate, 12 – sensor for the outlet temperature for permeate, 13 – tank for permeate, 14 – membrane module, 15 – membrane

The following equation is used to calculate the permeate flux:

$$J_v = V \times \rho/A \times t \qquad (1)$$

where: J_v – the vapor diffusion rate (in kilograms per square meter per hour), V – the amount of water collected in liters, is the water density in kilograms per cubic meter, A – the effective surface area of the membrane in square meters, and t is the period in hours. The feed and permeate salt concentrations going into and coming out of the membrane module were measured using a conductivity meter (German-made Model DDS 307)(Ameen et al. 2020, Beauregard et al. 2020).

The following equation was used to determine the salt rejection:

$$R(\%) = [1 - (C_P/C_F)] \times 100 \qquad (2)$$

In which R is the rejection of salt concentration of the permeates solution (C_P) and concentration of the feed solution (C_F). This study analyzed the DCMD performance in two phases, with feed temperatures ranging from 35 to 55 °C. To carry out The major studies on desalinating salt water, we first tested the prepared membrane's performance of the one layer and double layer at different amounts, a feed at several temperatures (i.e., 35, 45, and 55 °C), using a feed flow rate of 0.6 L/min with feed salt concentrations at 70 g/L.

The permeate flux data showed that (25PAN:75PMMA) membranes were the best option for preparation. Three operating parameters were used to evaluate further the water vapor flux, each with three different setups. Table 1 summarizes the results of nine experiments with varying parameters to meet the Taguchi technique's minimum and maximum requirements for experiment selection. The number of tests is shown by the nine rows, while the studied parameters at three levels each are represented by the three columns. Next, a set of minimal experiments was conducted using the Taguchi technique on membranes made from a mixture of 30% PMMA and 10% PAN (25PAN:75PMMA) at different feed temperatures (i.e., 35, 45, 55, and 65 °C), different feed salt concentrations (i.e., 70, 140, and 210 g/L), and different feed flow rates (i.e., 2, 0.4, and 0.6 L/min).

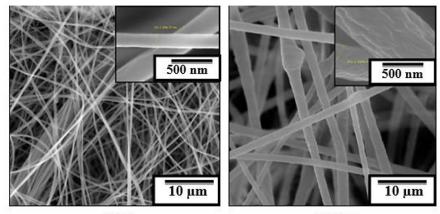## RESULTS AND DISCUSSION

Characterization of membranes

Figure 3 offers SEM graphs of the surface morphologies of the nanofiber membranes that were made with two layers of nonwoven material (PAN: PMMA) before DCMD experiments, in addition to scanning electron microscopy (SEM) pictures of the manufactured pure 30 wt% PMMA/DMF and

Table 1. DCMD experimentals using Taguchi technique requirements

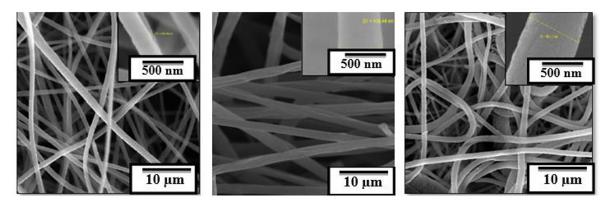| Run	Feed temperature T (C°)	Feed concentration C (g/L)	Feed flow rate F (L/min)
1	35	70	0.2
2	35	140	0.4
3	35	210	0.6
4	45	70	0.4
5	45	140	0.6
6	45	210	0.2
7	55	70	0.6
8	55	140	0.2
9	55	210	0.4

Figure 2. The membrane module from the outside and inside

PAN   PMMA

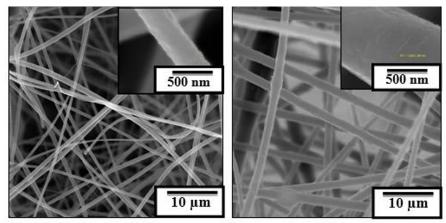PAN:PMMA (75:25)   PAN:PMMA (50:50)   PAN:PMMA (25:75)

Figure 3. SEM of double-layer nonwoven nanofiber membranes (PAN: PMMA)
that were prepared before MD experiments with the thickness (10 µm)

pure 10 wt% PAN/DMF based nonwoven nanofibers membranes. Images showed that membranes comprised 30 wt% PMMA/DMF and 10 wt% PAN/DMF contained homogeneous and continuous nanofibers with average fiber sizes of 1055.7 and 254.17 nm before DCMD processing. Broad, brittle PMMA fibers with a big fiber and pore size needed to be enhanced by joining them with fibers with a small fiber and pore size, similar to PAN's pure nonwoven nanofiber membrane. Membrane layers of different sizes were seen, with smaller PAN-based fibers appearing at the bottom and bigger PMMA-based fibers forming a continuous top layer. The ratio of PMMA in the dual-layer membrane influences the number of large fibers present in the membrane. Increasing the ratio of PMMA results in an increase in the number of large fibers (Waisi 2021). Fiber size increases from 254.17 nm for pure PAN to 328.66 nm for 75PAN:25PMMA, 438.44 nm for 50PAN:50PMMA, an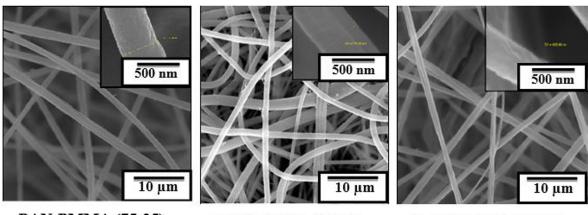d 613.52 nm for 25PAN:75PMMA, all while maintaining the same total thickness. All of the prepared (pure and double layer) membranes, before and after the DCMD procedure, were suitable for the MD system based on the average fiber diameters. In terms of both change and rejection, the outcomes were uniformly positive.

The membrane's suitable pores and hydrophobic nature in MD cause doesn't need pressure on the membrane that causes fouling on the walls compared to reverse osmosis RO. However, little pore or fiber size expansion at high temperatures leads to modest wetting. After MD experiments, the double-layer membranes made from PAN and PMMA nonwoven nanofibers may be seen under a scanning electron microscope in Figure 4. After going through the DCMD procedure, the average fiber diameter of the PMMA/DMF (30 wt%) and PAN/DMF (10 wt%) membranes increased to 1223.59 and 414.66 nm, respectively, as seen in the photos. Average fiber diameters acceptable for MD increased to 436.8, 534.68, and 678.08 nm,

Figure 4. SEM of double-layer nonwoven nanofiber membranes (PAN: PMMA) that were prepared after MD experiments with thickness (10 μm)

respectively, after being expanded in a hot solution for a variety of nanofiber membranes made of two-layer materials (PAN: PMMA) (25:75), (50:50), and (75:25).

Figure 5 also compares the measured water contact angles before and after MD. The best values for hydrophobicity acceptable for MD were found in all membranes made using nanofibers, and this success was recorded. Contact angles were greatest for the (25 PAN: 75 PMMA) nanofiber membrane, which is very hydrophobic. Therefore, a hydrophobic dual-layer nanofiber membrane (about 137.8°) was produced by spinning a layer of very hydrophobic nanofibers made with PMMA (136.2°) on the layer of highly hydrophobic PAN-based nanofibers (110.1°).

In the same membrane, the generated water-repellent nanofibers improved hydrophobicity, preventing the membrane from becoming wet. With its superior hydrophobicity, the PAN nanofiber membrane achieved the lowest value. In contrast, the PMMA-based nanofiber membrane had the greatest contact angle (Waisi, et al. 2019) because of its strong hydrophobicity. Hydrophobic dual-layer nanofiber membranes

with PAN: PMMA ratios of 75:25 (around 120°), 50:50 (around 126.3°), and 25:75 (around 137.8°) were produced by spinning nanofibers made of very hydrophobic polymethyl methacrylate (136.2°) on top of a layer of highly hydrophobic PAN-based nanofibers (110.1°). Hydrophobic and hydrophobic nanofibers in a single membrane prevented water from entering the holes by forcing it into the micro and rough structure, instead collecting saline droplets inside the hydrophobic fibers. Table 2 shows the characterizations of prepared membranes before and after membrane distillation. The mechanical properties are better and more robust, and there is less wetting because of the percentage increase in fiber size expansion and the percentage decrease in contact angle at N_4.

Membrane efficiency in distillation process

The prepared membranes' results are summarized in Table 3; there, it is observed that (N_1 and N_5) membrane have a high flux despite their high conductivity and concentration and low rejection compared to the other membranes.
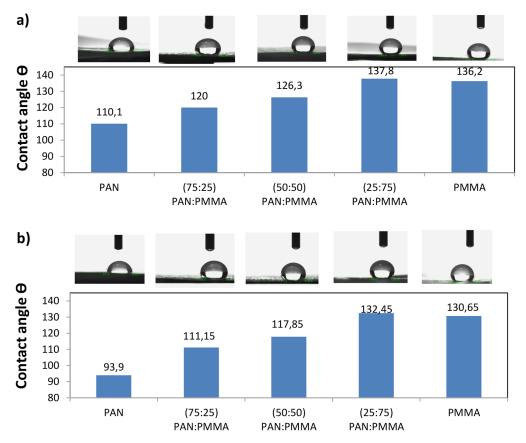

Figure 5. Contact angle of the obtained double-layers (PAN: PMMA) membranes of nanofibers nonwoven before and after MD experiments (a) before MD (b) after MD

Table 2. The characterizations of the prepared membranes

Polymer Wt.%	Membrane name	Fiber size before MD	Fiber size after MD	Increase in fiber size %	Contact angle before MD	Contact angle after MD	Decrease in contact angle %
PAN 100%	N_1	254.17	414.66	39	110.1	93.9	17.25
75 PAN:25 PMMA	N_2	328.66	436.80	25	120	111.15	7.9
50 PAN:50 PMMA	N_3	438.44	534.68	18	126.3	117.85	7.2
25 PAN:75 PMMA	N_4	613.52	678.08	9.5	137.7	132.45	4
PMMA 100%	N_5	1055.7	1223.59	14%	136.2	130.65	4.2

Table 3. The distillation efficiency in the DCMD process of prepared membranes (70 g/L feed concentration at 55 °C temperature of the feed and 0.6 L/min the rate of feed flow

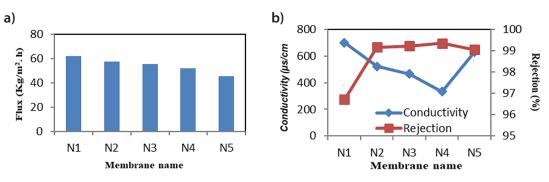| Membrane name	Flux (kg/m²·h)	Concentration (g/L)	Conductivity (μs/cm)	Rejection %
N_1	61.761	2.3	701	96.714
N_2	57.312	0.57	523	99.176
N_3	55.331	0.54	466	99.223
N_4	51.872	0.45	334	99.356
N_5	45.138	0.660	634	99.057

Figure 6. Influence of different membranes on (a) flux, (b) conductivity, and rejection at 70 g/L feed concentration at 55 °C temperature of the feed and 0.6 L/min the rate of feed flow

However, (N_4) membrane produced water of lower conductivity, salt concentration, and higher in rejection with very close rates in flux with N_2 and N_3. This is illustrated in Figure 6. The best ideal membrane was determined to be an N_4 in (25PAN:75PMMA) preparation, and this membrane was tested using the DCMD system and the Taguchi method.

The Taguchi technique was developed as a strong statistical framework strategy to improve manufacturing product quality. It has been employed to plan experiments to investigate the effects of different factors on the standard deviation and value of any parameter measuring process performance used to evaluate the process's efficacy. The method relies on the an effective experimental design (DOEs) to reduce process variance (Safi, et al. 2020).

An $L_9(3^3)$ using three levels of orthogonal array variables was studied using the Taguchi method. Table 4 displays the experimental results for the flux and rejection produced membrane at (25 PAN:75 PMMA). Almost 180 minutes had passed before the flow could be measured. As performance qualities improve, so does permeate flux. Table 4 displays how the DCMD procedure's permeate flux is affected by each parameter.

The orthogonality of the experiment allowed us to separate the influence of individual operating parameters on the overall effect (permeate flux) across a range of linear values. The constructed membrane response values are displayed in Table 4. The optimal working conditions for these studies (higher performance characteristic) were 70 g/L, 0.6 L/min, and 55 °C, as evidenced by the highest penetrate flux of 51.872 (kg/m²·h) for the constructed membrane. The average permeation

Table 4. Taguchi L9(3³) orthogonal array, and the conclusions from studies carried out on prepared membrane (M₂). At 70 g/L feed concentration, 55 °C the temperature of feed, and 0.6 L/min the rate of feed flow

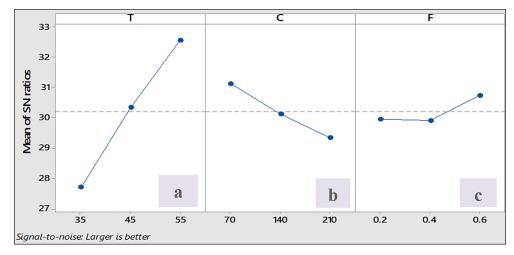| Run	Feed temperature T (ºC)	The concentration of feed C (g/L)	The rate of feed flow F (L/min)	Flux (kg/m²·h)	Rejection %
1	35	70	0.2	25.671	99.527
2	35	140	0.4	24.070	99.491
3	35	210	0.6	23.142	99.450
4	45	70	0.4	34.982	99.433
5	45	140	0.6	33.917	99.421
6	45	210	0.2	29.972	99.392
7	55	70	0.6	51.872	99.356
8	55	140	0.2	40.489	99.330
9	55	210	0.4	36.394	99.270

Figure 7. Effect of operating variables on mean of means: (a) feed temperature; (b) concentration (c) feed flow rate

flux values from each experiment run are used to illustrate the main effect plots. We observe that the mean of means has raised with increasing the temperature of feed and the rate of feed flow, consistent with the average reasonable permeate flux under the specified operating parameters as shown by the imaginary line. Figure 7 shows that this value dropped as feed concentration increased. Each operating condition parameter's effect on the permeate flux has been accounted for in the figure. The permeate flux was found to be most affected by the temperature of feed and least affected by the rate of feed flow. Using the statistical software package "Minitab" version17, the ability to calculate the flux of permeation in relation to the operational variables and generate an empirical correlation, the temperature of feed (T), the rate of feed flow (F), and the concentration of feed (C) as following regression equation with R-sq = 95.34%:

$$Flux = -5.11 + 0.931T - 0.0548C + 10.67F \quad (3)$$

CONCLUSIONS

Highly organically permeable dual-layer nanofiber membranes were successfully created in this work by means of electrospinning. Hydrophobic PMMA nanofibers were spun as a top layer on top of a hydrophobic PAN nanofiber membrane to create the manufactured membrane. Characterization of the manufactured membranes revealed that the PMMA nanofiber layer's spinning significantly impacted the PAN base layer regarding fiber size and wettability. Using a DCMD system, the various membranes were put through their paces in membrane distillation desalination. Dual-layer nanofiber membranes achieved high rejection, decreased wetting resistance, and increased permeate flux. Several concentrations of the flat membrane sheet were successfully manufactured and used in DCMD membrane distillation. The effectiveness of N₄

has been vastly enhanced. A conductivity of around 334 µs/cm and rejection of 99.356%, the best permeate flux (51.872 kg/m²·h) was gained by a 70 g/L solution at 55 °C the temperature of feed and 0.6 L/min the rate of feed flow. The temperature of feed increasing, the rate of feed flow decreasing, and increasing in NaCl content, resulted in a higher permeation flux. The permeation flux is primarily affected by the temperature of feed and least by the rate of feed flow.

REFERENCES

1. Al-Furaiji, M., Kadhom, M., Kalash, K., Waisi, B., Albayati, N. 2020. Preparation of thin-film composite membranes supported with electrospun nanofibers for desalination by forward osmosis. Drink. Water Eng. Sci., 13(2), 51–57. https://doi.org/10.5194/dwes-13-51-2020

2. Al-Alawy, A.F., Al–Musawi, M.S. 2013. Microfiltration membranes for separating oil / water emulsion. Iraqi Journal of Chemical and Petroleum Engineering, 14(4), 53–70. https://ijcpe.uobaghdad.edu.iq/index.php/ijcpe/article/view/326

3. Alkarbouly, S., Waisi, B. 2022, January. Dual-layer Antifouling Membrane of Electrospun PAN: PMMA Nonwoven Nanofibers for Oily Wastewater Treatment. In Proceedings of 2nd International Multi-Disciplinary Conference Theme: Integrated Sciences and Technologies, IMDC-IST 2021, 7–9 September 2021, Sakarya, Turkey.

4. Alkhudhiri, A., Darwish, N., Hilal, N. 2012. Membrane distillation: a comprehensive review. Desalination, 287, 2–18. https://doi.org/10.1016/j.desal.2011.08.027

5. Ameen, N.A.M., Ibrahim, S.S., Alsalhy, Q.F., Figoli, A. 2020. Highly saline water desalination using direct contact membrane distillation (DCMD): Experimental and Simulation Study. Water, 12(6).

6. Beauregard, N., Al-Furaiji, M., Dias, G., Worthington, M., Suresh, A., Srivastava, R. et al. 2020. Enhancing iCVD Modification of electrospun membranes for membrane distillation using a 3d printed scaffold. Polymers, 12(9), 2074. https://doi.org/10.3390/polym12092074

7. Cheng, D., Gong, W., Li, N. 2016. Response surface modeling and optimization of direct contact membrane distillation for water desalination. Desalination, 394, 108–122. https://doi.org/10.1016/j.desal.2016.04.029

8. Cheryan, M., Rajagopalan, N. 1998. Membrane processing of oily streams. Wastewater treatment and waste reduction. Journal of Membrane Science, 151(1), 13–28. https://doi.org/https://doi.org/10.1016/S0376-7388(98)00190-2

9. Eleiwi, F., Ghaffour, N., Alsaadi, A.S., Francis, L., Laleg-Kirati, T.M. 2016. Dynamic modeling and experimental validation for direct contact membrane distillation (DCMD) process. Desalination, 384, 1–11. https://doi.org/https://doi.org/10.1016/j.desal.2016.01.004

10. Fard, A.K., Manawi, Y. 2014. Seawater desalination for production of highly pure water using a hydrophobic PTFE membrane and direct contact membrane distillation (DCMD). Int. J. Environ. Chem. Ecol. Geol. Geophys. Eng, 8, 398–406.

11. Francis, L., Venugopal, J., Prabhakaran, M.P., Thavasi, V., Marsano, E., Ramakrishna, S. 2010. Simultaneous electrospin–electrosprayed biocomposite nanofibrous scaffolds for bone tissue regeneration. Acta Biomaterialia, 6(10), 4100–4109. https://doi.org/https://doi.org/10.1016/j.actbio.2010.05.001

12. Guo, F., Servi, A., Liu, A., Gleason, K.K., Rutledge, G.C. 2015. Desalination by membrane distillation using electrospun polyamide fiber membranes with surface fluorination by chemical vapor deposition. ACS Applied Materials & Interfaces, 7(15), 8225–8232. https://doi.org/10.1021/acsami.5b01197

13. Haghighat Bayan, M.A., Afshar Taromi, F., Lanzi, M., Pierini, F. 2021. Enhanced efficiency in hollow core electrospun nanofiber-based organic solar cells. Scientific Reports, 11(1), 21144. https://doi.org/10.1038/s41598-021-00580-4

14. Hameed, K.W. 2013. Concentration of orange juice using forward osmosis membrane process. Iraqi Journal of Chemical and Petroleum Engineering, 14(4), 71–79. https://ijcpe.uobaghdad.edu.iq/index.php/ijcpe/article/view/327

15. Heikkilä, P., Harlin, A. 2008. Parameter study of electrospinning of polyamide-6. European Polymer Journal, 44(10), 3067–3079. https://doi.org/10.1016/j.eurpolymj.2008.06.032

16. Hu, X., Chen, X., Giagnorio, M., Wu, C., Luo, Y., Hélix-Nielsen, C., Yu, P., Zhang, W. 2022. Beaded electrospun polyvinylidene fluoride (PVDF) membranes for membrane distillation (MD). Journal of Membrane Science, 661, 120850. https://doi.org/10.1016/j.memsci.2022.120850

17. Khalaf, A.S., Hassan, A.A. 2019. A comparison study of brine desalination using direct contact and air gap membrane distillation. Journal of Engineering, 25(11), 47–54. https://doi.org/10.31026/j.eng.2019.11.04

18. Li, B., Cui, Y., Chung, T.S. 2019. Hydrophobic perfluoropolyether-coated thin-film composite membranes for organic solvent nanofiltration. ACS Applied Polymer Materials, 1(3), 472–481. https://doi.org/10.1021/acsapm.8b00171

19. Li, Y., He, Y., Zhuang, J., Shi, H. 2022. An intelligent natural fibrous membrane anchored with ZnO

for switchable oil/water separation and water purification. Colloids and Surfaces A: Physicochemical and Engineering Aspects, 634, 128041. https://doi.org/10.1016/j.colsurfa.2021.128041

20. Majeed, B.A.A., Zubaidy, M.A. 2016. Performance study of electrodialysis for treatment fuel washing wastewater. Iraqi Journal of Chemical and Petroleum Engineering, 17(4), 35–42.

21. Meng, L., Wang, L., Wang, Z. 2023. Membrane distillation with electrospun omniphobic membrane for treatment of hypersaline chemical industry wastewater. Desalination, 564, 116782. https://doi.org/10.1016/j.desal.2023.116782

22. Rashad, Z. 2022. Studying and analyzing operating conditions of hollow fiber membrane preparation process: a review paper. Iraqi Journal of Chemical and Petroleum Engineering, 23(2), 47–53. https://doi.org/10.31699/IJCPE.2022.2.7

23. Sabeeh, H., Waisi, B.I. 2022. Effect of solvent type on PAN–Based nonwoven nanofibers membranes characterizations. Iraqi Journal of Chemical and Petroleum Engineering, 23(4), 43–48. https://doi.org/10.31699/IJCPE.2022.4.6

24. Safi, N.N., Ibrahim, S.S., Zouli, N., Majdi, H.S., Alsalhy, Q.F., Drioli, E., Figoli, A. 2020. A systematic framework for optimizing a sweeping gas membrane distillation (SGMD). Membranes, 10(10), 254. https://www.mdpi.com/2077-0375/10/10/254

25. Shalaby, T., Hamad, H., Ibrahim, E., Mahmoud, O., Al-Oufy, A. 2018. Electrospun nanofibers hybrid composites membranes for highly efficient antibacterial activity. Ecotoxicology and Environmental Safety, 162, 354–364. https://doi.org/https://doi.org/10.1016/j.ecoenv.2018.07.016

26. Sheraz, M., Ly, H.N., Thi Le, V.C., Nguyen, V.Q., Naqvi, F.H., Park, J.Y., Lee, H., Kim, S., Lee, W.R., Parasuraman, V. 2023. Electrospinning synthesis of CuBTC/TiO2/PS composite nanofiber on HEPA filter with self-cleaning property for indoor air purification. Process Safety and Environmental Protection, 172, 621–631. https://doi.org/https://doi.org/10.1016/j.psep.2023.02.047

27. Shukla, S., Benes, N.E., Vankelecom, I., Méricq, J.P., Belleville, M.P., Hengl, N., Marcano, J.S. 2015. Sweep gas membrane distillation in a membrane contactor with metallic hollow-fibers. Journal of Membrane Science, 493, 167–178. https://doi.org/https://doi.org/10.1016/j.memsci.2015.06.040

28. Waisi, B.I. 2019. Carbonized copolymers nonwoven nanofibers composite: surface morphology and fibers orientation. Iraqi Journal of Chemical and Petroleum Engineering, 20(2), 11–15. https://doi.org/10.31699/IJCPE.2019.2.2

29. Waisi, B.I., Al-Jubouri, S.M., McCutcheon, J.R. 2019. Fabrication and characterizations of silica nanoparticle embedded carbon nanofibers. Industrial & Engineering Chemistry Research, 58(11), 4462–4467. https://doi.org/10.1021/acs.iecr.8b05825

30. Wang, R., Liu, Y., Li, B., Hsiao, B.S., and Chu, B. 2012. Electrospun nanofibrous membranes for high flux microfiltration. Journal of Membrane Science, 392–393, 167–174. https://doi.org/10.1016/j.memsci.2011.12.019

31. Woo, Y.C., Yao, M., Shim, W.G., Kim, Y., Tijing, L.D., Jung, B., Kim, S.H., Shon, H.K., 2021. Co-axially electrospun superhydrophobic nanofiber membranes with 3D-hierarchically structured surface for desalination by long-term membrane distillation. Journal of Membrane Science, 623, 119028. https://doi.org/https://doi.org/10.1016/j.memsci.2020.119028

32. Zhou, W., Wang, R.A., Joy, L.D. 2006. Fundamentals of scanning electron microscopy (SEM), In Scanning microscopy for nanotechnology,. Springer New York. https://doi.org/10.1007/978-0-387-39620-0_1